Desalination and Water Treatment
www.deswater.com

doi: 10.5004/dwt.2018.22224

110 (2018) 109–116
April

Photo-catalytic inactivation of *E. coli* using stabilized Ag/S, N-TiO_2 nanoparticles by fixed bed photo-reactor under visible light and sunlight

Neda Masoudipour, Mehraban Sadeghi*, Fazel Mohammadi-Moghadam

Department of Environmental Health Engineering, School of Health, Shahrekord University of Medical Sciences, Rahmatieh, Shahrekord, Iran, Tel. + 98 38 333346712; Fax +98 38 333334678; emails: sadeghi@skums.ac.ir (M. Sadeghi), n.masoudipour@yahoo.com (N. Masoudipour), fazel.health@gmail.com (F. M.-Moghadam)

Received 23 September 2017; Accepted 9 March 2018

ABSTRACT

Silver (Ag), sulfur (S), and nitrogen (N)-codoped titanium dioxide (TiO_2) photo-catalysts were prepared by sol-gel method. The main compounds were tetrabutyl orthotitanate, 250 mg of thiourea, and 0.7, 1.4, and 2.8 mg of silver nitrate as the suppliers of sulfur, nitrogen, and silver, respectively. These photo-catalysts were stabilized on glass microbeads. The structural properties of synthesized photo-catalysts were investigated by X-ray diffraction, scanning electron microscopy, and energy dispersive X-ray. The optical activity of the photo-catalysts was evaluated by UV/Vis diffuse reflectance spectroscopy. Finally, the feasibility of inactivation of *Escherichia coli*, an index of water contamination, was investigated by the stabilized photo-catalyst in a fixed bed photo-reactor under visible light and sunlight. We observed that Ag (0.14 mg)/S, N-TiO_2 caused 99.6% removal of *E. coli* at 1.5×10^8 CFU/mL initial concentration under visible light, but this photo-catalyst caused approximately 97% removal of *E. coli* under sunlight. These findings would help to better use the fixed bed reactor filled with stabilized photo-catalysts such as Ag/S, N-TiO_2, as a multipurpose and efficient technique to disinfect waters highly contaminated with *E. coli*.

Keywords: Photo-catalysis; Sunlight; Visible light; Fixed bed photo-reactor; Bacterial disinfection; Ag, S, and N-codoped TiO_2

1. Introduction

Because of rapid growth in industry, population, and drought, drinking water shortage is considered a serious problem in the world [1,2]. Nowadays, certain substances, such as chlorine, ozone, and UV radiation are used to disinfect drinking water in the final step of water treatment. However, the use of chlorine leads to production of carcinogenic and mutagenic substances, and the use of UV radiation or ozone is highly costly [3]. An important strategy to overcome such problems is using of semiconductor-based photo-catalysis that produces powerful OH and superoxide radicals for non-selective destruction of organic pollutants to water and carbon dioxide [4–6]. In this heterogeneous photo-catalytic process, irradiation of a semiconductor by UV or visible light, excite the semiconductor and produces electrons in its conduction band (C_b) and holes in its valence band (V_b). The photogenerated electrons and holes (e/h pairs) can react with dissolved oxygen and water/hydroxyl to produce OH and superoxide radicals, respectively [7–9]. A widely used semiconductor is titanium dioxide (TiO_2, with band gap energy of 3.2 eV) photo-catalyst that can play an alternative or supplementary role in water treatment processes. It is a non-toxic and low-cost catalyst that can be used repeatedly without a decline in its photo-catalytic activity or production of dangerous by-products [10–13]. However, titanium dioxide has some drawbacks in photo-catalysis processes. First, its anatase phase (acts as the photo-catalyst) is able to absorb ultraviolet rays (4% of the sunlight), that is not cost-effective. Second, fast recombination of e/h pairs decreases its activity [14]. This can be happen for all mono-component semiconductor photo-catalysts [15]. In general, to overcome these problems different techniques including coupling of two or

* Corresponding author.

more semiconductors [16–19], supporting the semiconductors on suitable supports such as glass microbeads, glass fibers, silica, zeolites, and nanotubes [20–29], doping of some metals have been used [30–33]. Such modifying techniques may shift the absorption edge of semiconductors to longer wavelengths because of formation of mixed energy levels between the semiconductors [34,35].

A well-known noble metal dopant is silver because of its low cost and easy use that can increase the production of reactive oxygen species (Eqs. (1) and (2)) [36]. Therefore, this metal is used as an antibacterial agent and has long been used in healthcare. Ag ions are able to affect the bacterial electron transport chains and DNA replication [37]. Cell wall is the main constituent of a microorganism's structure and most intracellular compounds are organic. Contact with these highly oxidizing compounds can lead to damage to the microorganisms [38].

$$Ag^{+} + \cdot O_2^{-} \rightarrow Ag + O_2 \quad (1)$$

$$Ag + \cdot O_2^{-} \rightarrow Ag^{+} + O_2^{2-} \quad (2)$$

In recent years, increasing efforts are being made to fixed photo-catalysts on certain above mentioned beds because of some problems including the need for constantly stirring solution during study, costly filtering, and centrifugation of the solutions to recover the powder, distribution of the nanoparticles in the solution, and light blocking [39–41]. For this goal, different reactors have been studied for photo-catalytic treatment of water, including parabolic trough reactor, thin-film fixed bed reactors (as the most common reactor), compound parabolic collecting reactor, and double-skin sheet reactor [42–44].

In this study, we synthesized TiO_2 using sol-gel process, an ideal approach to produce metal oxides because of producing a homogeneous and highly pure product, and then limited its absorption in the visible light spectrum, decelerated the electron–hole recombination, and intensified the TiO_2 antibacterial activity using S, N, and Ag codoping. Afterwards, Ag/S, N-TiO_2 nanoparticles were placed on the bed of glass microbeads to be isolated rapidly and conveniently, and finally as a main aim of this work, the removal of *E. coli*, an index of drinking water microbial contamination, was investigated in the isolated fixed bed reactor under visible light and sunlight.

2. Materials and methods

2.1. Synthesizing of the photo-catalysts and supporting on the glass microbeads

All the chemicals used in this study were purchased from Merck Co. (Germany). A water distillation device (GFL, Germany) was used to prepare deionized water. TiO_2 sol was prepared by hydrolyzing tetrabutyl orthotitanate (TBOT) in an acidic solution. According to this method, 2.50 mL TBOT, 10 mL ethanol, and 2.50 mL acetyl acetone were mixed and after 30 min, a transparent, yellow solution was developed. Then, 2 mL deionized water was added into the solution and the solution was stirred for 10 min. To regulate sol pH at approximately 1.8, concentrated hydrochloric acid and sodium hydroxide were used. To supply S and N, 250 mg thiourea was added to the solution and then three different amounts (0.7, 1.4, and 2.8 mg) of silver nitrate were separately introduced. After 2 h, a stable, yellow sol was developed. To stabilize the sol, the glass microbeads, 450–550 μm in diameter, were used. First, the glass microbeads were washed with a washing solution, then placed in diluted hydrochloric acid for 8 h, washed with deionized water, and dried in a 105°C oven. Then, the microbeads were plunged into the solution. The microbeads, covered with photo-catalyst, were placed in the oven at 60°C for 4 h and the ethanol evaporated. At the end, the film stabilized on the microbeads was calcinated in furnace at 500°C for 10 h to convert to anatase phase. Finally, five photo-catalysts, TiO_2, S, N-TiO_2, Ag (0.7 mg)/S, N-TiO_2, Ag (1.4 mg)/S, N-TiO_2, and Ag (2.8 mg)/S, N-TiO_2, stabilized on the glass microbeads, were prepared [45,46].

2.2. Investigating the photo-catalysts' properties

The energy band gaps of the samples were investigated by UV/Vis diffuse reflectance spectroscopy (DRS) using a spectrophotometer (UV-1800, Shimadzu, Japan). Polymorphs types and the size of the nanocrystals of the five photo-catalysts on the glass microbeads were studied by X-ray diffraction (XRD) using Phillips X'pert Pro Multipurpose diffractometer at $2\theta = 10°–80°$. The surface morphology of the TiO_2 films was observed on scanning electron microscopy (SEM) (EVO"15, Zeiss, Germany) equipped with an energy dispersive X-ray (EDX) for elemental analysis.

2.3. Photo-catalytic inactivation of E. coli

To investigate the photo-catalytic inactivation of *E. coli*, the *E. coli* with genotype DH1 was studied. The bacteria were cultured on MacConkey agar growth medium. The growth medium was left at 37°C for 48 h to grow the bacteria. To investigate the photo-catalytic removal efficiency of the bacteria, the *E. coli* suspension was prepared at 10^8 colony-forming unit (CFU)/mL concentration. To achieve the desired number of bacteria, a 0.5 McFarland standard was used. According to this method, the absorbance read by spectrophotometer at 625 nm wavelength was expected to range between 0.08 and 0.13. This absorbance rate is equal to 1.5×10^8 CFU/mL bacteria [47]. Therefore, the bacterial suspension was partially introduced to 200 mL deionized water, such that the bacterial absorbance at 625 nm wavelength was equal to the absorbance of 0.5 McFarland standard. The reactor used in this study had five glass tubes, 200 mm high and 8 mm in diameter, filled with 50 g photo-catalyst stabilized on the glass microbeads and placed on a mirror which was fixed on a wooden support. 200 mL of the prepared bacterial suspension, with 200 mL/min flow rate, rotated in the reactor using a peristaltic pump. Synthetic photo-catalyst was able to undergo a series of experiments. The filled glass tubes were irradiated with visible light (400 W lamp) and sunlight (clear sky in autumn) in two series of the experiments while the distance was 10 cm between the glass tubes and the lamp. All the containers, photo-catalysts, and reactor connections were completely sterilized and all the experiments and samplings were conducted under sterile conditions. Fig. 1 illustrates

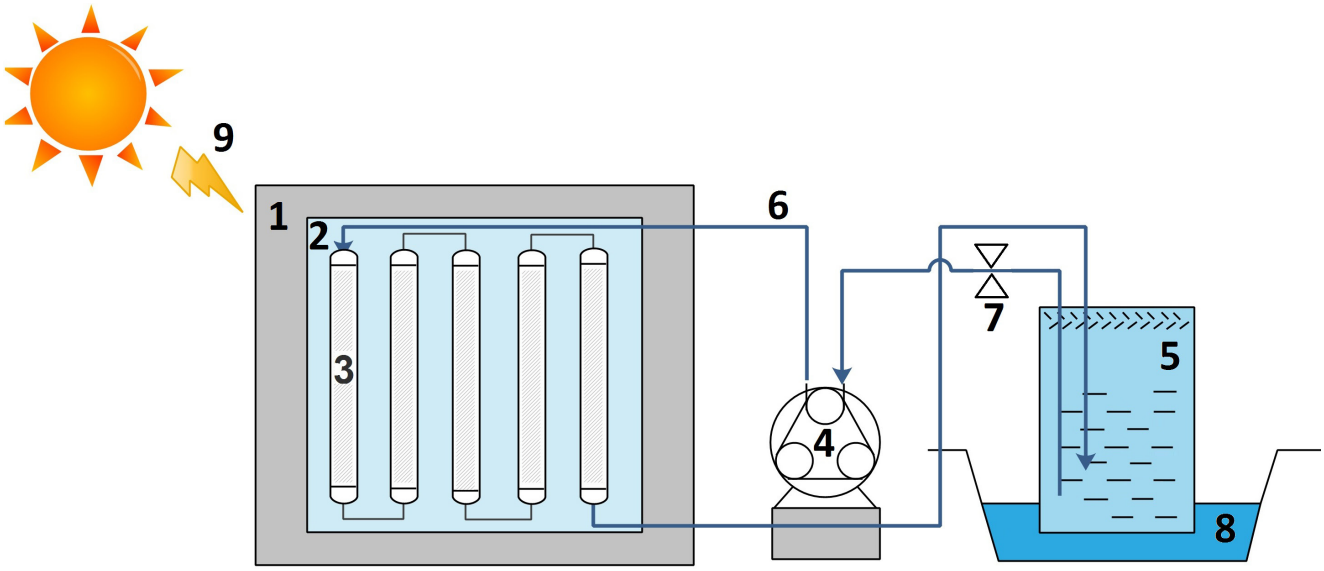

Fig. 1. Fixed bed reactor used in this study under sunlight; 1: wooden support; 2: mirror 3: photo-catalyst-contained glass tubes; 4: peristaltic pump; 5: isolated bacterial suspension-contained container; 6: silicon tubes; 7: sampling valve, 8: water bath, 9: the sun.

the fixed bed photo-reactor used to test the photo-catalytic removal of *E. coli* under sunlight. Each 30 min, 1 mL of the bacterial suspension was taken from sampling valve and introduced to a test tube containing 99 mL deionized water. Then, 0.01 mL of the solution was taken out of the test tube by a micropipette and placed in nutrient agar growth medium at 37°C for 24 h. For all the experiments, the pH was 7.

The variables of this study were time intervals (30, 60, 90, and 120 min), different photo-catalysts, consisting of TiO_2, S, N-TiO_2, and Ag/S, N-TiO_2, different amounts of Ag in the Ag/S, N-TiO_2 photo-catalyst, and the type of radiation (400 W lamp and the sun). All the experiments were conducted in duplicate and the mean rates were reported. To determine the rigor of the experiments, the standard deviations were also calculated. To calculate the photo-catalysts' efficiencies of the *E. coli* removal, Eq. (3) was used:

$$E.coli\ \text{photocatalytic removal}(\%)=\frac{(C_0-C)}{C_0}\times 100 \quad (3)$$

C_0 = CFU/mL initial; C = CFU/mL final.

3. Results and discussion

3.1. Morphological, compositional, and structural characterizations

Figs. 2(A)–(C) illustrate the XRD patterns of the films of TiO_2, S, N-TiO_2, and Ag (1.4 mg)/S, N-TiO_2 photo-catalysts, respectively. The peaks corresponding to *hkl* planes of 101, 004, 200, 105, 211, 204, 116, and 200, designated as *A* in all patterns, indicated that the diffraction of TiO_2 anatase phase corresponded to the standards of the diffraction no. 04-0477 of the Common Committee of the Powders Diffraction [48]. Anatase phase is the best crystallographic status of TiO_2 for

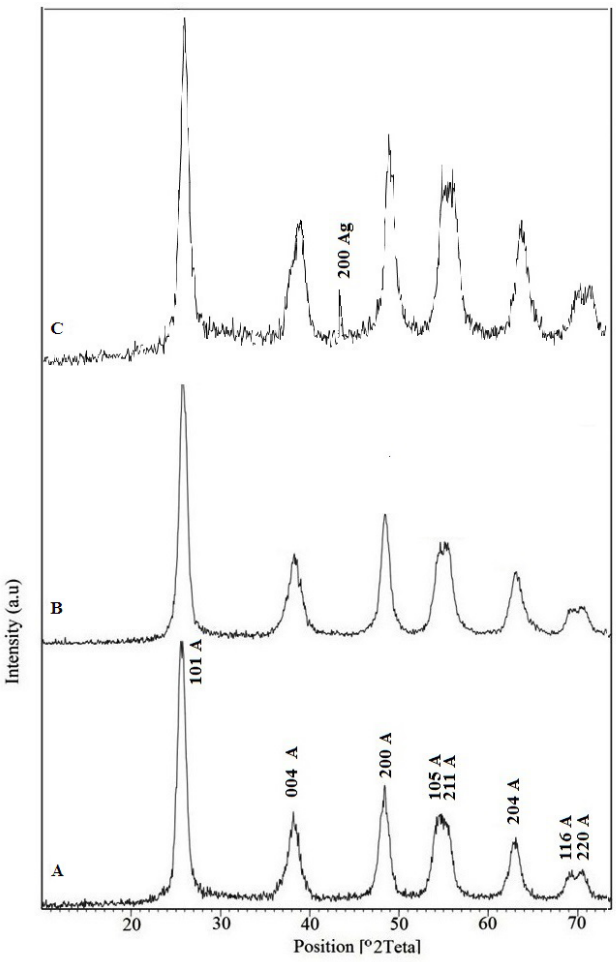

Fig. 2. X-ray diffraction pattern of the films ((A) TiO_2, (B) S, N-TiO_2; and (C) Ag [1.4 mg]/S, N-TiO_2) on the glass microbeads.

optical activity. No peaks were seen for N and S in Fig. 2(B) because of their low concentrations and adequate distribution in the anatase phase. But, in Fig. 2(C), only one peak (no. 200) was seen for Ag diffraction and no shift was seen for the peaks of TiO_2. Lack of Ag peaks in Fig. 2(C) can be explained by overlapping with the TiO_2 peaks of anatase phase.

The mean crystal size of the three photo-catalysts was approximately 10 nm on the glass microbeads by Scherrer equation [49] and using the peak 101 in $2\theta = 25.5°$. Therefore, adding thiourea and Ag caused no effect on the changes in the crystals' sizes.

Figs. 3(A)–(C) illustrate the SEM images of the films of TiO_2, S, N-TiO_2, and Ag (1.4 mg)/S, N-TiO_2 on the glass microbeads. The nanometric sizes of the particles could be clearly seen on the glass microbeads in all the three films. Overall, the photo-catalysts' nanometric particles are likely to accumulate because of Van der Waals attraction among the particles' surfaces [35]. Increased thiourea caused accumulation of TiO_2 particles (Fig. 3(B)), which became clearer after Ag addition (Fig. 3(C)).

The EDX analysis of Ag (1.4 mg)/S, N-TiO_2 film on glass microbead is shown in Fig. 4. This pattern has confirmed the presence of nitrogen, sulfur, and silver in Ag/S, N-TiO_2 film.

3.2. Optical properties of the photo-catalysts

Fig. 5(A) illustrates the DRS spectra of TiO_2, S, N-TiO_2, and Ag (0.7, 1.4, and 2.8 mg)/S, N-TiO_2 photo-catalysts. Although the common equation (Eq. (4)) has been used for the calculation of band gap energy of semiconductors (E_g is the band gap [eV] and λ is the wavelength [nm] of the absorption edges in the spectrum), the best method is Kubelka-Munk equation and Tauc plot [50–53].

$$E_g = \frac{1239.8}{\lambda} \tag{4}$$

In the following Kubelka-Munk and Tauc equations (Eqs. (5) and (6), respectively), K is the reflectance transformed according to Kubelka-Munk and R is the reflectance (%), E_g is the semiconductors' band gap (eV), h is Planck's constant (J s), ν is the frequency of light (Hz), β is the absorption constant. The absorption coefficient α is equal to $(2.303 \times \text{Abs.}/d)$ according to the Beer–Lambert's law, where d and Abs are the sample thickness and sample absorbance, respectively [54].

$$K = \frac{(1-R)^2}{2R} \tag{5}$$

$$(\alpha h\upsilon) = \beta(h\upsilon - E_g)^n \tag{6}$$

In this equation, n index has different values of 1/2, 2, 3/2, and 3 for allowed direct, allowed indirect, forbidden direct and forbidden indirect electronic transitions, respectively [55]. Typical plots for direct and indirect transitions are shown in Figs. 5(B) and (C). The band gaps were estimated by extrapolation of rising segments of plot to cross x-axis and the estimated values are shown in the figures.

As seen in Figs. 5(B) and (C), the band gap energies of TiO_2 are larger than the value of 3.2 eV. This can be explained because the band gap of semiconductors has been found to be particle size dependent and the band gap increases with decreasing particle size [56]. With increasing thiourea, the TiO_2 energy band gap was narrowed down because of mixing the non-metal p and TiO_2 oxygen 2p orbitals [57,58], and

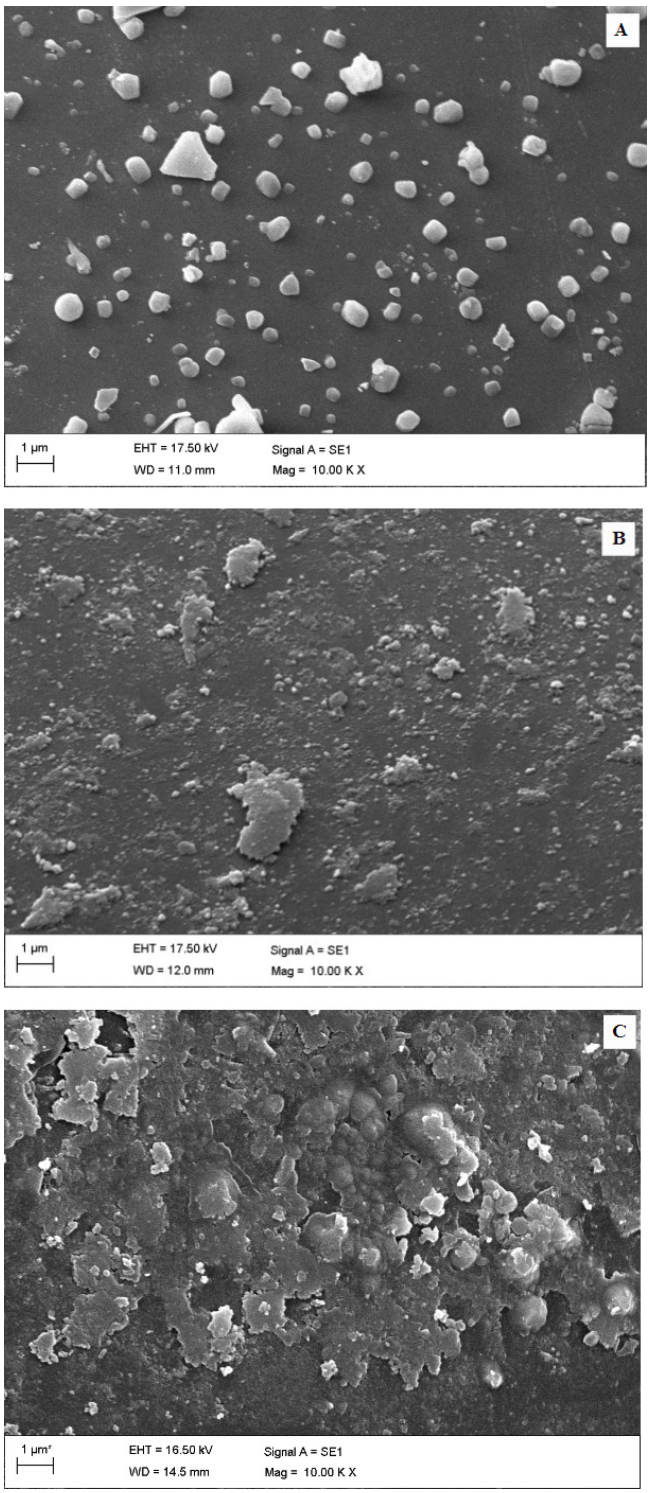

Fig. 3. Scanning electron microscopic images of the films ((A) TiO_2, (B) S, N-TiO_2, and (C) Ag [1.4 mg]/S, N-TiO_2) on the glass microbeads.

the optical response of the S, N-TiO_2 photo-catalyst entered into the visible spectrum. In addition, the Ag clusters in Ag/S, N-TiO_2 heightened the energy levels of the TiO_2 energy band gap, and the electrons of TiO_2 valence layer were excited at higher than 400 nm wavelengths. Indeed, S, N, and Ag codoping led to intensification of TiO_2 optical response in the visible spectrum.

3.3. Photo-catalytic inactivation of *E. coli*

Figs. 6(A)–(C) illustrate *E. coli* photo-catalytic removal rate in the vicinity of the five photo-catalysts films in the fixed bed reactor under dark, visible (lamp) light and sunlight, respectively. The maximum inactivation rate of *E. coli* in all photo-catalysts was obtained during a time interval of 120 min.

In Fig. 6(A), TiO_2 has shown low photo-catalytic activity in dark condition. After adding thiourea to TiO_2, the removal rate of bacteria has not substantially changed in dark condition but by adding Ag, the bacterial removal rate has increased approximately to 30%. By Ag/S, N-TiO_2, as the amount of silver increased from 0.7 to 2.8 mg, bacterial removal rate had an increasing trend from 20% to 40%.

In Fig. 6(B), under visible light, the bacterial removal rate with TiO_2 was gained approximately 20% more than dark condition. By adding thiourea, the bacterial removal rate was reached approximately to 50%. After adding Ag to TiO_2, the removal rate had a 30% increase compared with the TiO_2. In the presence of Ag/S, N-TiO_2, in the 1.4 mg silver, the bacterial removal rate reached to more than 99%.

By comparing Figs. 6(A) and (B) it can be seen that, unlike the darkness, in the presence of visible light, the greatest amount of silver has not shown the highest bacterial removal rate, so that, when the silver increased from 0.7 to 1.4 mg, the *E. coli* removal rate has enhanced but then it has decreased by raising the silver to 2.8 mg.

According to a study by Yuan et al. [36] under light, a large number of silver ions aggregate on the photo-catalyst and make large size granules, therefore these granules block transmitted light across photo-catalyst films and decrease the photo-catalytic activity of TiO_2. But in dark conditions, and by increasing silver, the antibacterial effect of silver plays the main role in *E. coli* removal.

According to Fig. 5(C), under sunlight the results were almost identical to visible light. The only difference is that, in all five photo-catalysts, the removal rate of *E. coli* was lower in general. Almost the same results were obtained in similar studies. Because first, silver ions on the surface of TiO_2 improve the separation of the photo-generated electrons and holes, and second silver ions prevent electron–hole recombination. On the other hand, silver ions increase OH

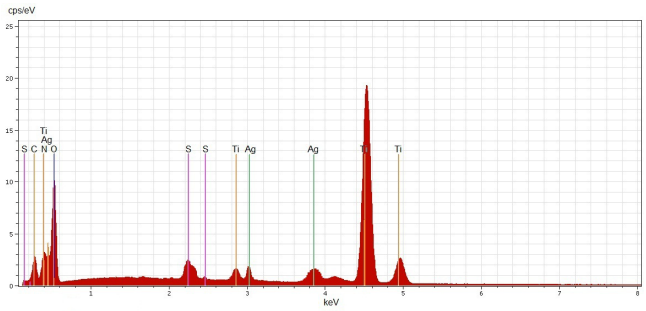

Fig. 4. EDX analysis of film of Ag (1.4 mg)/S, N-TiO_2 on glass microbeads.

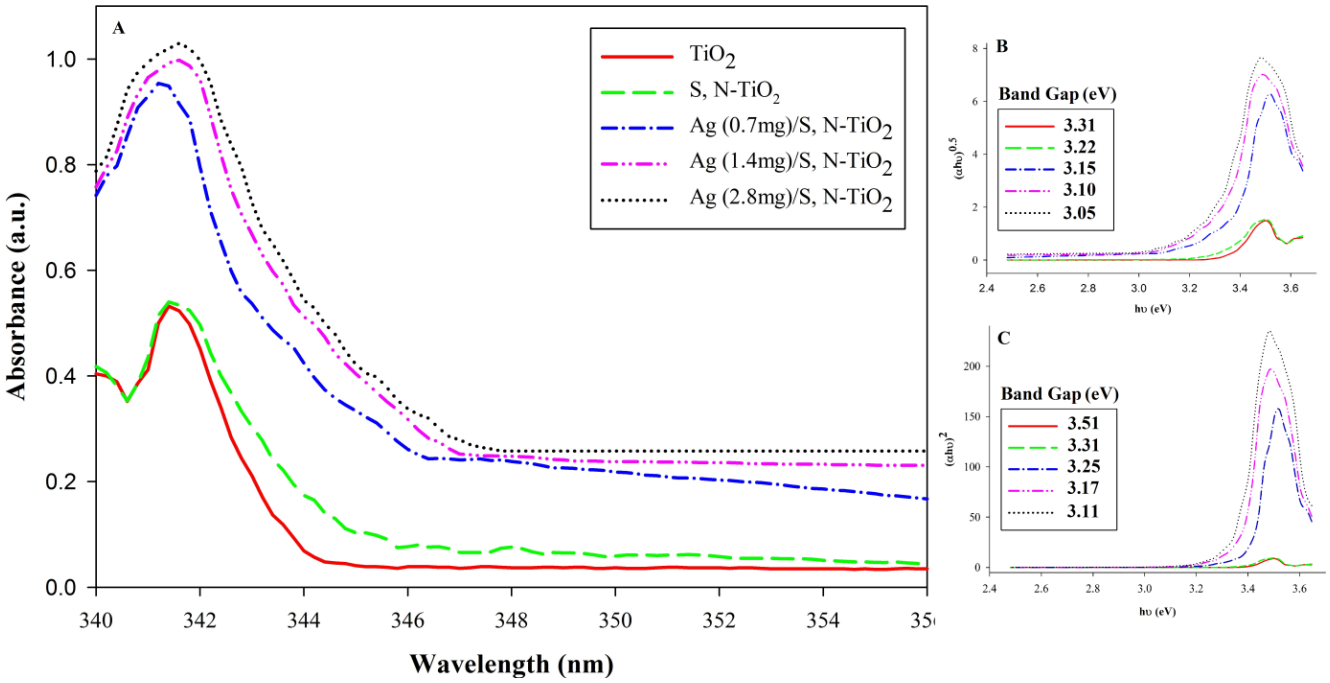

Fig. 5. (A) UV/Vis reflectance spectra of different photo-catalysts on the glass microbeads; typical Tauc plots for (B) indirect, and (C) direct transitions of the catalyst.

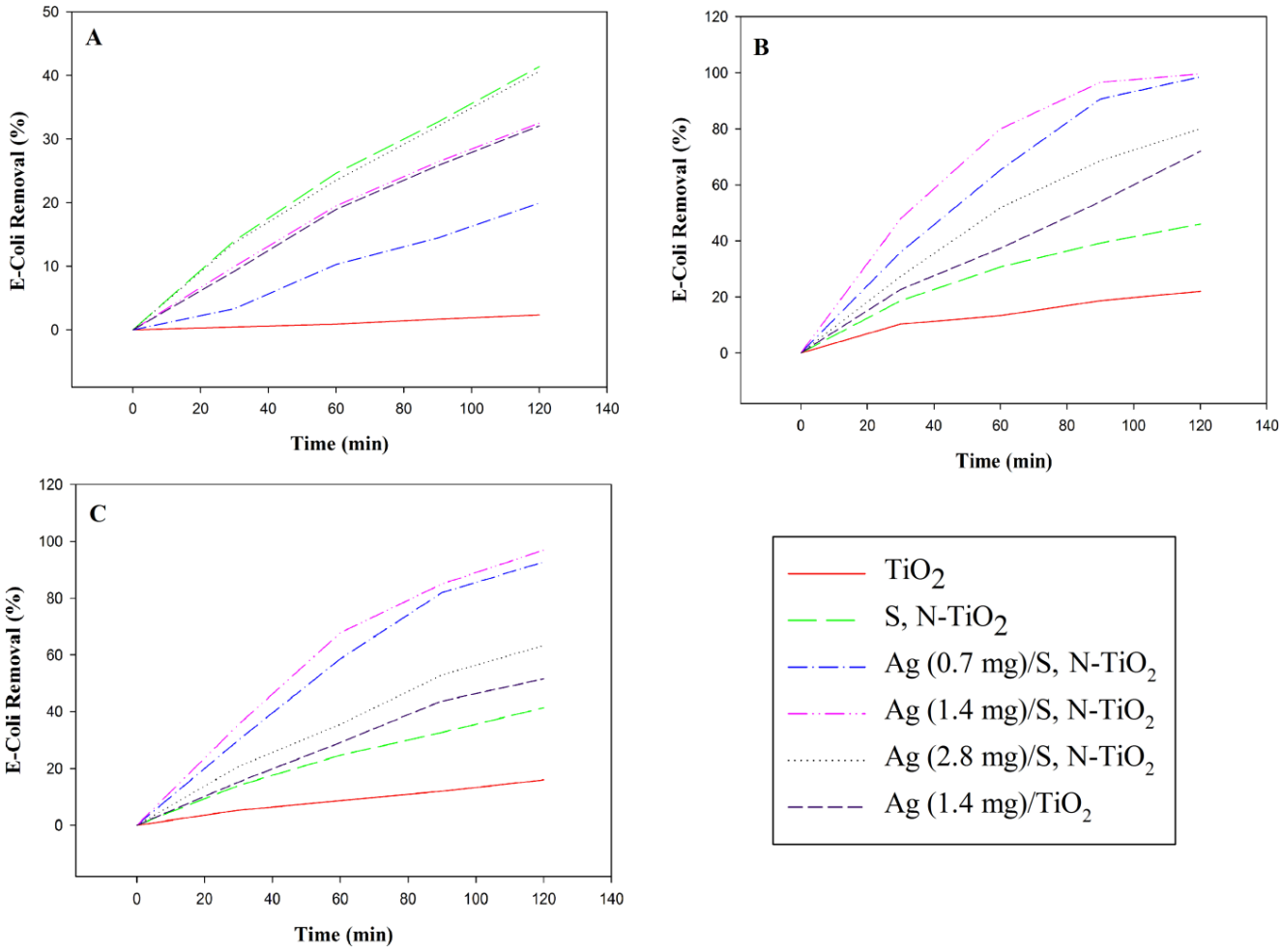

Fig. 6. *Escherichia coli* inactivation under ((A) dark, (B) visible light, and (C) sunlight) using different photo-catalysts.

and O_2^- radicals on the surface of TiO_2 and they enhance the TiO_2 activity as an oxidizer. Also silver ion is known to have strong anti-bacterial effect [10,37,59].

As it was mentioned, Ag/S, N-TiO_2 has considerably increased photo-catalytic activity of TiO_2 for *E. coli* removing. Gao et al. [24] also has found the same results in color removing. In fact, silver nanoparticles doped on S, N-TiO_2 delay S and N escape during the processes, and on the other hand according to the results presented in section 3.2, presence of Ag, S, and N all together has strengthened optical response of photo-catalyst.

When we compare visible light with sunlight in bacterial removal, the average removal rate of *E. coli* in sunlight was 6%–8% less than visible light. Sunlight is composed of two factors: heat (infrared photons) and UV–Vis photons; however, due to doing tests in partially cloudy and cloudy sky in winter, the intensity and also the heat of emitted light on the reactor was low, therefore the *E. coli* removal rate decreased in the sunlight.

4. Conclusion

Regarding the findings of this study, we can conclude that the use of fixed bed reactors, filled with stabilized photo-catalysts such as Ag/S, N-TiO_2, may be a multipurpose and efficient technique to disinfect waters highly contaminated with *E. coli*, as the most important index of water contamination. This conclusion may be explained by non-toxicity of the photo-catalyst and light source, relatively low cost, repeatability of the use of photo-catalyst, minimum risk of leakage of the photo-catalyst in water, and most importantly, high efficiency to remove the bacteria. Production of these photo-reactors in industrial scale for drinking water disinfection in disaster-afflicted or lowly populous areas is an implication of this study's findings.

Acknowledgement

The authors gratefully thank the Research and Technology Deputy of the Shahrekord University of Medical Sciences for funding this study.

References

[1] S.-H. Do, Y.-H. Jo, H.-D. Park, S.-H. Kong, Synthesis of iron composites on nano-pore substrates: identification and its application to removal of cyanide, Chemosphere, 89 (2012) 1450–1456.

[2] S. Hashemi, A. Nezamzadeh-Ejhieh, A novel chromium selective electrode based on surfactant-modified Iranian clinoptilolite nanoparticles, Desal. Wat. Treat., 57 (2016) 3304–3314.
[3] X. Dai, P.L. Breuer, Cyanide and copper cyanide recovery by activated carbon, Miner. Eng., 22 (2009) 469–476.
[4] P. Raizada, J. Kumari, P. Shandilya, P. Singh, Kinetics of photocatalytic mineralization of oxytetracycline and ampicillin using activated carbon supported ZnO/$ZnWO_4$ nanocomposite in simulated wastewater, Desalination, 79 (2017) 204–213.
[5] B.A. Ünnü, G. Gündüz, M. Dükkancı, Heterogeneous Fenton-like oxidation of crystal violet using an iron loaded ZSM-5 zeolite, Desal. Wat. Treat., 57 (2016) 11835–11849.
[6] M. Karimi-Shamsabadi, A. Nezamzadeh-Ejhieh, Comparative study on the increased photoactivity of coupled and supported manganese-silver oxides onto a natural zeolite nano-particles, J. Mol. Catal. A: Chem., 418–419 (2016) 103–114.
[7] M. Giahi, A. Hoseinpour Dargahi, Photocatalytic degradation of phenylephrine hydrochloride in aqueous solutions by synthesized SnO_2-doped ZnO nanophotocatalyst, Iran. J. Catal., 6 (2016) 381–387.
[8] P.-C. Maness, S. Smolinski, D.M. Blake, Z. Huang, E.J. Wolfrum, W.A. Jacoby, Bactericidal activity of photocatalytic TiO_2 reaction: toward an understanding of its killing mechanism, Appl. Environ. Microbiol., 65 (1999) 4094–4098.
[9] F. Mohammadi-Moghadam, M. Sadeghi, N. Masoudipour, Degradation of cyanide using stabilized S, N-TiO_2 nanoparticles by visible and sun light, J. Adv. Oxid. Technol., 21 (2018).
[10] S. Murgolo, F. Petronella, R. Ciannarella, R. Comparelli, A. Agostiano, M.L. Curri, G. Mascolo, UV and solar-based photocatalytic degradation of organic pollutants by nano-sized TiO_2 grown on carbon nanotubes, Catal. Today, 240 (2015) 114–124.
[11] S.L. Gora, S.A. Andrews, Adsorption of natural organic matter and disinfection byproduct precursors from surface water onto TiO_2 nanoparticles: pH effects, isotherm modelling and implications for using TiO_2 for drinking water treatment, Chemosphere, 174 (2017) 363–370.
[12] A. Besharati-Seidani, Photocatalytic oxidation of an organophosphorus simulant of chemical warfare agent by modified TiO_2 nanophotocatalysts, Iran. J. Catal., 6 (2016) 447–454.
[13] H. Zabihi-Mobarakeh, A. Nezamzadeh-Ejhieh, Application of supported TiO_2 onto Iranian clinoptilolite nanoparticles in the photodegradation of mixture of aniline and 2, 4-dinitroaniline aqueous solution, J. Ind. Eng. Chem., 26 (2015) 315–321.
[14] A.N. Ejhieh, M. Khorsandi, Photodecolorization of Eriochrome Black T using NiS–P zeolite as a heterogeneous catalyst, J. Hazard. Mater., 176 (2010) 629–637.
[15] S.N. Frank, A.J. Bard, Heterogeneous photocatalytic oxidation of cyanide and sulfite in aqueous solutions at semiconductor powders, J. Phys. Chem., 81 (1977) 1484–1488.
[16] M. Bahrami, A. Nezamzadeh-Ejhieh, Effect of supporting and hybridizing of FeO and ZnO semiconductors onto an Iranian clinoptilolite nano-particles and the effect of ZnO/FeO ratio in the solar photodegradation of fish ponds waste water, Mater. Sci. Semicond. Process., 27 (2014) 833–840.
[17] V.K. Gupta, A. Fakhri, M. Azad, S. Agarwal, Synthesis and characterization of Ag doped ZnS quantum dots for enhanced photocatalysis of Strychnine asa poison: charge transfer behavior study by electrochemical impedance and time-resolved photoluminescence spectroscopy, J. Colloid Interface Sci., 510 (2018) 95–102.
[18] A. Nezamzadeh-Ejhieh, M. Bahrami, Investigation of the photocatalytic activity of supported ZnO–TiO_2 on clinoptilolite nano-particles towards photodegradation of wastewater-contained phenol, Desal. Wat. Treat., 55 (2015) 1096–1104.
[19] J. Esmaili-Hafshejani, A. Nezamzadeh-Ejhieh, Increased photocatalytic activity of Zn(II)/Cu(II) oxides and sulfides by coupling and supporting them onto clinoptilolite nanoparticles in the degradation of benzophenone aqueous solution, J. Hazard. Mater., 316 (2016) 194–203.
[20] C. Zhao, B. Feng, Y. Li, J. Tan, X. Lu, J. Weng, Preparation and antibacterial activity of titanium nanotubes loaded with Ag nanoparticles in the dark and under the UV light, Appl. Surf. Sci., 280 (2013) 8–14.
[21] Z.-A. Mirian, A. Nezamzadeh-Ejhieh, Removal of phenol content of an industrial wastewater via a heterogeneous photodegradation process using supported FeO onto nanoparticles of Iranian clinoptilolite, Desal. Wat. Treat., 57 (2016) 16483–16494.
[22] T. Ohno, M. Akiyoshi, T. Umebayashi, K. Asai, T. Mitsui, M. Matsumura, Preparation of S-doped TiO_2 photocatalysts and their photocatalytic activities under visible light, Appl. Catal., A, 265 (2004) 115–121.
[23] N. Ajoudanian, A. Nezamzadeh-Ejhieh, Enhanced photocatalytic activity of nickel oxide supported on clinoptilolite nanoparticles for the photodegradation of aqueous cephalexin, Mater. Sci. Semicond. Process., 36 (2015) 162–169.
[24] Y. Gao, P. Fang, F. Chen, Y. Liu, Z. Liu, D. Wang, Y. Dai, Enhancement of stability of N-doped TiO_2 photocatalysts with Ag loading, Appl. Surf. Sci., 265 (2013) 796–801.
[25] A. Bagheri Ghomi, V. Ashayeri, Photocatalytic efficiency of $CuFe_2O_4$ by supporting on clinoptilolite in the decolorization of acid red 206 aqueous solutions, Iran. J. Catal., 2 (2012) 135–140.
[26] A. Nezamzadeh-Ejhieh, Z. Ghanbari-Mobarakeh, Heterogeneous photodegradation of 2,4-dichlorophenol using FeO doped onto nano-particles of zeolite P, J. Ind. Eng. Chem., 21 (2015) 668–676.
[27] M. Karimi-Shamsabadi, M. Behpour, A.K. Babaheidari, Z. Saberi, Efficiently enhancing photocatalytic activity of NiO-ZnO doped onto nanozeoliteX by synergistic effects of p-n heterojunction, supporting and zeolite nanoparticles in photo-degradation of Eriochrome Black T and Methyl Orange, J. Photochem. Photobiol., A, 346 (2017) 133–143.
[28] S. Landi, J. Carneiro, S. Ferdov, A.M. Fonseca, I.C. Neves, M. Ferreira, P. Parpot, O.S.G.P. Soares, M.F.R. Pereira, Photocatalytic degradation of Rhodamine B dye by cotton textile coated with SiO_2-TiO_2 and SiO_2-TiO_2-HY composites, J. Photochem. Photobiol.. A, 346 (2017) 60–69.
[29] H. Derikvandi, A. Nezamzadeh-Ejhieh, Increased photocatalytic activity of NiO and ZnO in photodegradation of a model drug aqueous solution: effect of coupling, supporting, particles size and calcination temperature, J. Hazard. Mater., 321 (2016) 629–638.
[30] S. Sato, R. Nakamura, S. Abe, Visible-light sensitization of TiO_2 photocatalysts by wet-method N doping, Appl. Catal., A, 284 (2005) 131–137.
[31] H. Fallah Moafi, Photocatalytic self-cleaning properties of lanthanum and silver co-doped TiO_2 nanocomposite on polymeric fibers, Iran. J. Catal., 6 (2016) 281–292.
[32] H.R. Pouretedal, M. Fallahgar, F. Sotoudeh Pourhasan, M. Nasiri, Taguchi optimization of photodegradation of yellow water of trinitrotoluene production catalyzed by nanoparticles TiO_2/N under visible light, Iran. J. Catal., 7 (2017) 317–326.
[33] Y. Cong, J. Zhang, F. Chen, M. Anpo, Synthesis and characterization of nitrogen-doped TiO_2 nano photocatalyst with high visible light activity, J. Phys. Chem. C, 111 (2007) 6976–6982.
[34] H. Derikvandi, A. Nezamzadeh-Ejhieh, Designing of experiments for evaluating the interactions of influencing factors on the photocatalytic activity of NiS and SnS_2: focus on coupling, supporting and nanoparticles, J. Colloid Interface Sci., 490 (2017) 628–641.
[35] G. Laera, B. Jin, H. Zhu, A. Lopez, Photocatalytic activity of TiO_2 nanofibers in simulated and real municipal effluents, Catal. Today, 161 (2011) 147–152.
[36] Y. Yuan, J. Ding, J. Xu, J. Deng, J. Guo, TiO_2 nanoparticles co-doped with silver and nitrogen for antibacterial application, J. Nanosci. Nanotechnol., 10 (2010) 4868–4874.
[37] V. Rodríguez-González, S.O. Alfaro, L. Torres-Martínez, S.-H. Cho, S.-W. Lee, Silver–TiO_2 nanocomposites: synthesis and harmful algae bloom UV-photoelimination, Appl. Catal., B, 98 (2010) 229–234.
[38] V. Augugliaro, V. Loddo, G. Marcì, L. Palmisano, M.a.J. López-Muñoz, Photocatalytic oxidation of cyanides in aqueous titanium dioxide suspensions, J. Catal., 166 (1997) 272–283.

[39] H.-Y. Chun, S.-S. Park, S.-H. You, Gi-Hyeon, W.-T. Bae, K.-W. Kim, J. Park, A. Ozturk, D.-W. Shin, Preparation of a transparent hydrophilic TiO_2 thin film photocatalyst, J. Ceram. Process Res., 10 (2009) 219–223.
[40] Q. Zhang, H. Wang, X. Fan, F. Lv, S. Chen, X. Quan, Fabrication of TiO_2 nanofiber membranes by a simple dip-coating technique for water treatment, Surf. Coat. Technol., 298 (2016) 45–52.
[41] H. Khalilian, M. Behpour, V. Atouf, S.N. Hosseini, Immobilization of S, N-codoped TiO_2 nanoparticles on glass beads for photocatalytic degradation of methyl orange by fixed bed photoreactor under visible and sunlight irradiation, Sol. Energy, 112 (2015) 239–245.
[42] Y. Wu, H. Yuan, X. Jiang, G. Wei, C. Li, W. Dong, Photocatalytic degradation of 4-tert-octylphenol in a spiral photoreactor system, J. Environ. Sci., 24 (2012) 1679–1685.
[43] M. Noorjahan, M. Pratap Reddy, V. Durga Kumari, B. Lavédrine, P. Boule, M. Subrahmanyam, Photocatalytic degradation of H-acid over a novel TiO_2 thin film fixed bed reactor and in aqueous suspensions, J. Photochem. Photobiol., A, 156 (2003) 179–187.
[44] T. Ochiai, A. Fujishima, Photoelectrochemical properties of TiO_2 photocatalyst and its applications for environmental purification, J. Photochem. Photobiol., C, 13 (2012) 247–262.
[45] M. Behpour, M. Chakeri, Ag-doped TiO_2 nanocomposite prepared by sol gel method: photocatalytic bactericidal under visible light and characterization, J. Nanostruct., 2 (2012) 227–234.
[46] M. Behpour, V. Atouf, Study of the photocatalytic activity of nanocrystalline S, N-codoped TiO_2 thin films and powders under visible and sun light irradiation, Appl. Surf. Sci., 258 (2012) 6595–6601.
[47] K.C. Chapin, T.L. Lauderdale, Reagents, Stains, and Media: Bacteriology, ASM Press, Washington, D.C, 2003.
[48] T. Swanson, N.J.C. Fel, Reports, Private Communication, ICDD Powder Diffraction Database File Card Number [00-004-0551], 1950.
[49] L. Szpyrkowicz, S.N. Kaul, E. Molga, M. DeFaveri, Comparison of the performance of a reactor equipped with a Ti/Pt and an SS anode for simultaneous cyanide removal and copper recovery, Electrochim. Acta, 46 (2000) 381–387.
[50] M. Babaahamdi-Milani, A. Nezamzadeh-Ejhieh, A comprehensive study on photocatalytic activity of supported Ni/Pb sulfide and oxide systems onto natural zeolite nanoparticles, J. Hazard. Mater., 318 (2016) 291–301.
[51] H. Derikvandi, A. Nezamzadeh-Ejhieh, Synergistic effect of p-n heterojunction, supporting and zeolite nanoparticles in enhanced photocatalytic activity of NiO and SnO_2, J. Colloid Interface Sci., 490 (2017) 314–327.
[52] P. Kubelka, F. Munk, An article on optics of paint layers, Z. Tech. Phys., 12 (1931) 593–609.
[53] J. Tauc, R. Grigorovici, A. Vancu, Optical properties of electronic structure of amorphous germanium, Phys. Status Solidi, 15 (1966) 627–637.
[54] S. Jafari, A. Nezamzadeh-Ejhieh, Supporting of coupled silver halides onto clinoptilolite nanoparticles as simple method for increasing their photocatalytic activity in heterogeneous photodegradation of mixture of 4-methoxy aniline and 4-chloro-3-nitro aniline, J. Colloid Interface Sci., 490 (2017) 478–487.
[55] H. Derikvandi, A. Nezamzadeh-Ejhieh, A comprehensive study on enhancement and optimization of photocatalytic activity of ZnS and SnS_2: response surface methodology (RSM), n-n heterojunction, supporting and nanoparticles study, J. Photochem. Photobiol., A, 348 (2017) 68–78.
[56] R. Vijayalakshmi, V. Rajendran, Synthesis and characterization of nano-TiO_2 via different methods, Arch. Appl. Sci. Res., 4 (2012) 1183–1190.
[57] W. Qin, J. Qi, Y. Chen, H. Li, X. Wu, Visible light drived N, S-codoped TiO_2 photocatalysts grown by microplasma oxidation method, Int. J. Electrochim. Sci., 8 (2013) 7680–7686.
[58] J. Wang, H. Li, H. Li, C. Zou, Mesoporous TiO_2–xAy (A = N, S) as a visible-light-response photocatalyst, Solid State Sci., 12 (2010) 490–497.
[59] M. Sokmen, S. Degerli, A. Aslan, Photocatalytic disinfection of *Giardia intestinalis* and *Acanthamoeba castellani* cysts, Exp. Parasitol., 119 (2008) 44–48.